Prediction of elastic properties of cement pastes at early ages

Stefan Lavinia, Farid Benboudjema, Jean Michel Torrenti, Benoit Bissonnette

Prediction of elastic properties of cement pastes at early ages

Lavinia Stefan [a,b,*], Farid Benboudjema [a], Jean-Michel. Torrenti [a,c], Benoît Bissonnette [b]

[a] ENS Cachan/CNRS UMR8535/UPMC/PRES UniverSud Paris, 61 Avenue du Président Wilson, 94235 Cachan Cedex, France
[b] CRIB, Université Laval, Québec, Canada G1V 0A6
[c] LCPC, Paris, 58 Boulevard Lefebvre, 75732 Paris, France

Cementitious materials are known to be sensitive to cracking at early ages. During the first days which follow the contact between water and cement, the system is continuously evolving, as its mechanical characteristics follow a rapid rate of change and the material is prone to cracking. One of the parameters that highly influence the behavior of the material at early ages is the Young's modulus. Analytical calculations, based on existing homogenization models and finite element calculations, applied on a discrete generated microstructure, are first considered in order to predict the elastic properties of the material. As long as the cohesive role played by the hydrates is not taken into account, results at early age remain inaccurate, especially for low water–cement ratios. The need of modeling an intrinsic characteristic of cementitious materials – setting – arises. An approach, based on percolation and on the so-called "burning" algorithm, which takes into account explicitly the bonding role of hydrates and reveals a degree of hydration threshold below which the rigidity of the material is negligible, is therefore proposed. The evolution of the elastic characteristics is obtained by applying the previous computation methods to the percolation cluster given by the burning algorithm.

Keywords:
Cement paste
Early age
Elastic moduli
Microstructure
Modeling
Percolation

1. Introduction

Modeling the behavior of concrete at early age in order to predict its cracking potential can be a very delicate task, as a multitude of phenomena occur at this time. One of the main phenomena to address is the very complex nature of the hydration process. The hydration reaction is governed by the fact that the absolute volume of the hydration products is smaller than that of initial constituents, leading to the creation of internal voids (in a hardening system) [39]. At the macroscopic scale, especially for low w/c ratios, this translates into autogenous shrinkage. Provided the structure deformations are restrained, this will give rise to tensile stresses within the material, which can lead to cracking [38]. Moreover, the hydration reaction of the cement paste is highly exothermic so thermal strains will arise. If these strains are restrained, or if a strain gradient occurs between the skin and core of the structure, there is a considerable risk of cracking. In order to be able to control such cracking, the behavior of the material under certain given conditions needs to be thoroughly investigated and understood, in order to develop a predictive model of the stresses and strains that occur within the material.

The cracking risk depends to a large extent on the development of the mechanical properties at this stage. It is known that the rate of development of Young's modulus is faster than that of compressive and tensile strengths, reaching a significant fraction of its long-term value after only a few days [34,35]. The stresses that are generated in structures are closely related to the rapid development of the Young's modulus, which makes it an important parameter to be studied in order to better understand the behavior of the material. The change in Young's modulus as a function of the degree of hydration is a parameter that can be used to develop a predictive model of the early age behavior. In order to do this, a description of the porous space, a hydration model and a percolation approach are needed.

The prediction of the evolution of Young's modulus with the advancement of the hydration reaction is the subject of a number of studies. From a macroscopic point of view, the evolution of mechanical properties of early age cementitious materials can be associated to the degree of hydration. A phenomenological relationship between the Young's modulus and the degree of hydration was used by several authors [1–5]. The relationship makes use of the concept of percolation threshold (in terms of degree of hydration), which allows taking into account a particular characteristic of cementitious materials, namely setting. Still [6] showed that at very early ages, right after setting, the relationship does not predict with accuracy the evolution of the elastic properties of the material. Therefore, the authors proposed an improvement of the

* Corresponding author. Address: ENS Cachan/CNRS UMR8535/UPMC/PRES UniverSud Paris, 61 Avenue du Président Wilson, 94235 Cachan Cedex, France. Tel.: +33 0 6 21 57 48 39.
E-mail address: stefan@lmt.ens-cachan.fr (L. Stefan).

relation, by shifting the percolation threshold towards lower degrees of hydration.

Other macroscopic approaches are based on the maturity concept, and the development of Young's modulus in time is defined as a function of the final value of Young's modulus and the equivalent time, by means of an Arrhenius – like relationship [7].

More refined models [8,9] have been proposed to simulate a virtual hydrating cementitious system, providing important information on the microstructural development as the degree of hydration, the percolation threshold (notion intimately related to the setting phenomenon), the connected fraction of the solid or the volume fractions of the phases taken under consideration. These data are used as an input for models to predict the development of the mechanical properties.

A good correlation between experimental data and results obtained by elastic finite element calculations for composite materials is reported by Haecker et al. [10], mainly for degrees of hydration above 0.5. The volume fractions of the different phases were obtained using the NIST model [8]. A same type of approach has been applied on a leached mortar [11].

Using the input provided by another discrete hydration model [9,12] first modeled the cement paste with the bridging particle concept, and proposed a composite model of the microstructure (the "bar model"), which can be applied at the concrete scale. The bridging particle concept, proposed by van Breugel [9] states that the development of the mechanical properties is a function of the formation of contacts between particles during hydration, concept linked to the evolution of the connectivity between the solid phases [40]. The microstructure considered as divided into layers and bars, and the evolution of the hydrating microstructure is modeled by changing the properties of the elements defined (the layers and the bars that form the gel formed increase with the hydration). The information needed is generated by using the hydration model aforementioned [9]. However, the authors point out that the elastic modulus is overestimated for degrees of hydration that are lower than 0.2.

An interesting approach was made by Sun et al. [13], as the authors consider that as hydrates come into contact with the advancement of hydration, the contact area between the particles is the main parameter that determines the mechanical properties of the system. The authors also show the dependence between the percolation threshold and the water to cement ratio. This is consistent with the results that will be presented further on.

An analytical homogenization approach is proposed by Bernard et al. [5]. The authors consider the microstructure of the cementitious material at different levels, and a suited homogenization approach is applied at each level. However, for low w/c cement pastes, the model predicts non realistic values of Young's modulus at very early age. Sanahuja et al. [14] improved the prediction accuracy, by modifying the aspect ratio of C–S–H (ratio between the diameter parallel to the axis of revolution to a diameter perpendicular to the axis of revolution). By changing the morphology of the inclusions, which are generally considered sphere – shaped, they clearly illustrated a change in the response of the homogenization method used, in terms of percolation threshold and evolution of Young's modulus.

Analytical and numerical homogenization methods are compared by Šmilauer and Bittnar [15]. The input is given by the NIST model [8]. The authors show that numerical homogenization yields more accurate results.

The aim of this paper is to propose a simple alternative for the prediction of Young's modulus at early age. Percolation threshold is predicted only by taking into account explicitly the fact that hydrates act cohesively (i.e. like a glue) in the cement paste, as in [16]. A classical self-consistent scheme, with spherical particles is used and compared to 2D and 3D FEM. As in [14], Powers hydration model [17] is used here for the sake of simplicity but the approach can be used with more accurate hydration models (e.g. [8,9,37]).

2. Cement hydration model

As mentioned above, several complex hydration models already exist in the literature, two of the most used such models being Cemhyd3D [8] and Hymostruc [9]. Provided the adequate input is used for each model, the yielded results are very close [18].

Still, the purpose of the present work does not call for an accurate hydration model, one that describes with fidelity the complex nature of the microstructure of the cement paste. Different computational methods, applied on a simpler microstructure, can provide significant insight on the limits and advantages of each method. Results should be regarded from a qualitative point of view.

The hydration model used here was proposed by Powers [17] and further on used by several researchers (see for example [19,14]). The cement paste is composed of three phases: the anhydrous cement grains, the hydrates and the porosity. It is assumed that the hydrates occupy a volume 2.31 times larger than that of the reactants, leading to the following relationships:

$$V_{anh} \propto = \frac{V}{1+3.2\frac{W}{c}}(1-\propto) \tag{1}$$

$$V_{hyd} \propto = V\frac{1+1.13\propto}{1+3.2\frac{W}{c}} - V_{anh}(\propto) \tag{2}$$

$$V_{pore}(\propto) = V - V_{hyd}(\propto) - V_{anh}(\propto) \tag{3}$$

where V_{anh}, V_{hyd}, V_{pore} and V represent respectively the volume of anhydrous cement, the volume of hydration products, the volume of pores and the total volume of the system. w/c is the water to cement ratio and α is the degree of hydration. It is straightforward to calculate from this simple model the volume of each phase of a cement paste for a given water to cement ratio.

The initial microstructure (containing only anhydrous cement and pores for $\alpha = 0$) is first generated, by randomly distributing the solid particles on a 2D or 3D mesh. Next, for each value of degree of hydration, the volume fractions of each phase are computed using Eqs. (1)–(3), and the microstructure is modified accordingly, based on several rules. For each specifies increment of the degree of hydration, the volume fraction of anhydrous particles which have reacted and the volume fraction of newly formed hydrates are calculated (Eqs. (1) and (2)). Anhydrous particles which have reacted are replaced by hydrates (the anhydrous cement grains surrounded by the greatest number of water pixels hydrate first). Next, newly hydrated elements which remain to be distributed replace the water pixels (elements that are surrounded by the greatest number of anhydrous pixels). This process stops when a theoretical maximum degree of hydration α_{max} (function identified from experimental data) is reached [20]:

$$\alpha_{\max} = 1 - e^{(-3.3\cdot w/c)} \tag{4}$$

Typical 2D meshes are displayed in Fig. 1. The size of one pixel is 1 μm × 1 μm. The choice of the size of the representative elementary volume size is discussed later on.

3. Computation methods

In order to compute the elastic mechanical properties, two different approaches were taken into consideration and compared. In the first method, the generated digital images of the microstructure are directly imported to a finite element mesh. In the second case, a homogenization technique is used, assuming a particular morphology.

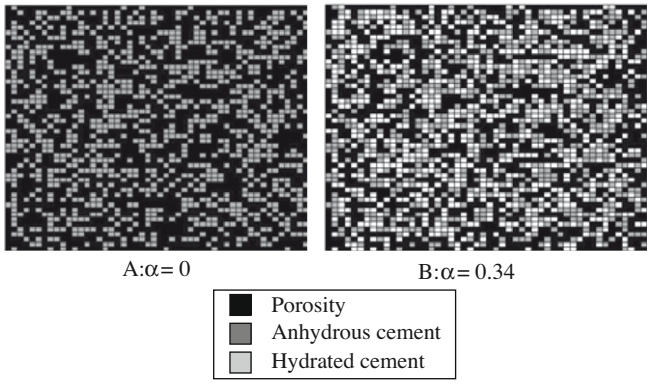

Fig. 1. Example of an initial randomly generated microstructure (A) and a hydrated microstructure (B) for $w/c = 0.50$ (in black the porosity; in grey the anhydrous cement; in white the hydrates).

3.1. Finite element computations

The digital images of the microstructures generated according to the method defined above, are exported to a finite element code [21], which recognizes every element found in the REV together with its respective given properties. The imported elements are initially quadrangular for the 2D calculus, and cubic for the 3D calculus. In order to study the influence of the mesh discretization, or the type of element on the results yielded, the automatic meshing tool provided by Cast3 m is used. It is considered that mechanical behavior law of all phases is elastic.

The displacement of the microstructure is blocked on the left-hand side (U_x) and at the bottom (U_y). The horizontal displacement at the right face is free, but identical in all nodes. The top side is subjected to a displacement U_{sup} (see Fig. 2). A typical mesh is also displayed in this figure, for $w/c = 0.35$ and $\alpha = 0.3$. The FE calculation is performed using Cast3m [21], which is a FE code developed by the CEA in France.

The elastic modulus of the different phases of the anhydrous cement was measured via nanoindentation techniques at the microscopic scale and via resonance frequencies techniques at the macroscopic scale by e.g. [22]. The elastic properties of the hydrates (C–S–H and CH) were obtained by Constantinides and Ulm [23], equally by performing nanoindentation tests. Data found in the literature (a mean value is considered for the anhydrous phases) and used as input in the proposed model are shown in Table 1. The porosity is assumed to be filled with water. It should be noted that results are identical whether one considers that porosity is filled with water or air, after mechanical percolation.

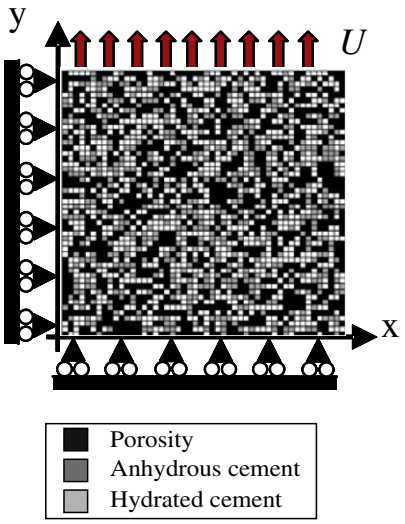

Fig. 2. Boundary conditions for numerical calculations and typical mesh of a cement paste ($w/c = 0.35$ and $\alpha = 0.3$).

3.2. Analytical computations

The determination of the elastic properties of composite materials is a classical mechanical problem. The work of Eshelby [24] was a starting point for other homogenization models that were developed. These homogenization models are able to predict the elastic properties of composite materials, providing the elastic properties, the morphologies and volume contents of each phase are given. Among them, two models are frequently applied in the case of cementitious materials.

The Mori–Tanaka scheme was successfully used by Bernard and coworkers [5,25]. The model, proposed by Benveniste [26] assembles the concept of average stress of Mori–Tanaka method with Eshelby's equivalent inclusion idea. However, at the scale of our model, the method cannot be applied. Not only it cannot capture the setting of the material, giving unrealistic results for low degrees of hydration [27], but it is difficult to evaluate in such a rapidly evolving microstructure which phase is to be considered as the matrix. Indeed, at very early age the matrix is formed by the mixing water, having the stiff cement grains and the softer hydrates as inclusions in a suspension. Once setting occurs, hydrates form, the water is consumed, porosity decreases and the matrix becomes now the hardening cement paste. Therefore, the use of Mori–Tanaka scheme at the cement paste scale leads to the decrease of Young's modulus with respect to degree of hydration [28].

The self-consistent scheme is closely related to the percolation theory, so it allows taking under consideration a percolation threshold, depending on the aspect ratio of the different phases [14]. It will however involve the solution of two nonlinear equations. The reference medium will be the homogenized medium, and the phases are disposed concentrically (see Fig. 3). This scheme gives good results in the case when it is difficult to make a distinction between the matrix and the inclusions in heteregenous materials. This is typically the case for the cement paste, as the respective volume fractions of the different phases evolve significantly with respect to time.

Homogenized bulk k_h and shear moduli g_h of the composite material are computed using the following equations [5]:

$$k_h = \sum_{i=1}^{i=n} f_i k_i \left[1 + \alpha_m \left(\frac{k_i}{k_h} - 1\right)\right]^{-1} \cdot \left[\sum_{i=1}^{i=n} f_i \left[1 + \alpha_m \left(\frac{k_i}{k_h} - 1\right)\right]\right]^{-1} \quad (5)$$

$$g_h = \sum_{i=1}^{i=n} f_i g_i \left[1 + \beta_m \left(\frac{g_i}{g_h} - 1\right)\right]^{-1} \cdot \left[\sum_{i=1}^{i=n} f_i \left[1 + \beta_m \left(\frac{g_i}{g_h} - 1\right)\right]\right]^{-1} \quad (6)$$

$$\alpha_m = \frac{3k_h}{3k_h + 4g_h} \quad (7)$$

$$\beta_m = \frac{6(k_h + 2g_h)}{5(3k_h + 4g_h)} \quad (8)$$

Table 1
Mechanical properties of each cement paste phase.

Anhydrous grains [21]		Hydrates [21]		Pores (filled with water)	
E (GPa)	υ	E (GPa)	υ	k^a (GPa)	g^b (GPa)
135	0.2	25	0.2	0	2.2

[a] Bulk modulus.
[b] Shear modulus.

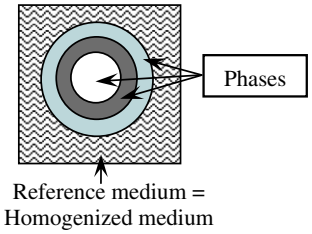

Fig. 3. Schematic representation of the self-consistent scheme.

where k_i and g_i are respectively the bulk and shear moduli of the phases taken into consideration in the model, f_i is the volumetric fraction of phase i, and α_m and β_m are function of the mechanical properties of the phases. This set of equation is solved iteratively using the Newton method.

4. Preliminary results

The results obtained with the two aforementioned methods (homogenization and finite element calculations) are presented in Figs. 4 and 5. In the case of finite element calculations (Fig. 4), it can be seen that for low water to cement ratio values, the Young's modulus has a non-zero value for a degree of hydration equal to 0. As the calculation is performed on the entire (non-percolated) microstructure, generated using the phase distribution as previously shown, the results can be regarded as valid only if the compressive behavior of the material is considered. Indeed, for low water to cement ratios, the solid fraction found in the microstructure is important enough to allow the material to exhibit some stiffness even before setting occurs. It is the case of a confined system for which the grain to grain contact governs its mechanical behavior in compression. Still, in the case of cementitious materials at early age, the interest lies mostly in their tensile behavior. A simple grain contact approach is not relevant, as it cannot account for cohesiveness of the system, which arises only upon setting. In that respect, the role played by the hydrates must be integrated into the model. A method that takes into account the cohesion provided by the hydrates was proposed by Torrenti and Benboudjema [16], with interface elements of zero thickness linking each pixel. Their tensile strength depends upon the properties of the neighbor particles. Still, this method leads to nonlinear finite element calculations, which are highly time-consuming.

Fig. 5 illustrates that the same problem emerges in the case of analytical computations. Bernard et al. [5] showed that the self-consistent scheme yields realistic results for high w/c ratio. However, they pointed out the existence of a critical w/c ratio for which the percolation threshold is equal to zero ($w/c = 0.318$), corresponding to a solid content equal to 0.5. Therefore, this scheme provides only good physical value, at early age, for w/c ratios greater than 0.318. Otherwise, a non-zero Young's modulus is predicted for $\alpha = 0$ for low w/c ratios. To solve this problem, [14] modified values for the hydrate aspect ratio. Another approach was used here, considering that hydrates act as a "glue", responsible for the development of cohesion. This is achieved by using the percolation theory, with slight modifications, as explained hereafter.

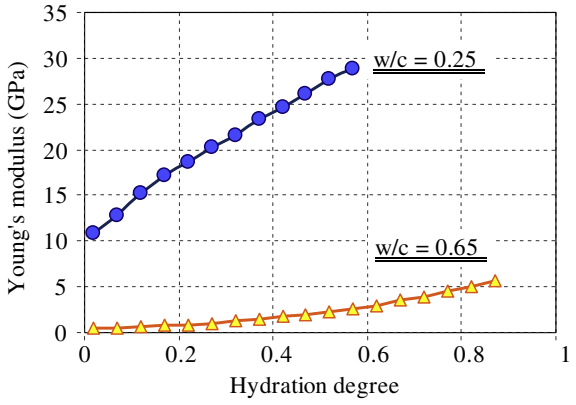

Fig. 4. FEM calculus: evolution of Young's modulus with respect to the degree of hydration (unpercolated microstructure).

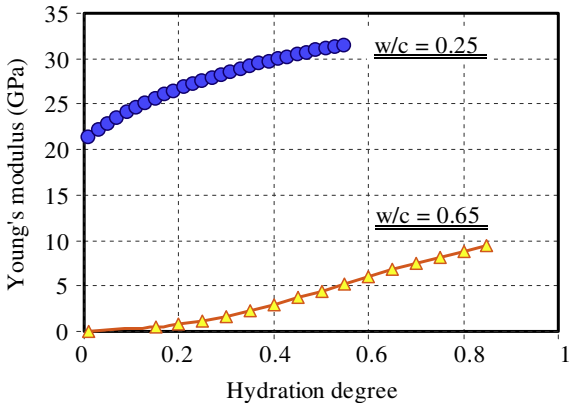

Fig. 5. Self-consistent scheme: evolution of Young's modulus with respect to the degree of hydration (unpercolated microstructure).

5. Percolation theory

Cementitious materials exhibit a sharp transition from fluid to solid at the setting time. It involves a threshold of the degree of hydration α_0 below which the strength and the Young's modulus of the material can be neglected. This behavior can be expressed by the relationship between the compressive strength f_c or the Young's modulus E_c and the degree of hydration [1–5]:

$$f_c(\alpha) = f_c(\alpha = \alpha_{\max}) \left\langle \frac{(\alpha - \alpha_0)}{\alpha_{\max} - \alpha_0} \right\rangle^{+} \tag{9}$$

$$E_c(\alpha) = \gamma \cdot f_c(\alpha)^{\beta} \tag{10}$$

$$E_c(\alpha) = E_c(\alpha = \alpha_{\max}) \cdot \left[\left\langle \frac{(\alpha - \alpha_0)}{\alpha_{\max} - \alpha_0} \right\rangle^{+} \right]^{\beta} \tag{11}$$

where α_{max} is the degree of hydration for which the hydration ceases and γ and β are material parameters which depends upon w/c, cement type, etc. From Eqs. (9)–(11) can be deduced. $\langle\rangle^{+}$ is the positive part operator.

Considering the relation between strength and the degree of hydration, the threshold α_0 is the intersection of the regression line of this relation and the x-axis. α_0, which is a genuine mechanical percolation threshold [29], plays therefore a key role in the prediction of generated stresses.

Below α_0, the stiffness is not equal to zero but can be neglected in the stress calculation. This percolation threshold refers here to the transition between the fluid and the solid states, which occurs at setting. It should be emphasized that the setting has several definitions, depending upon the method used to determine it experimentally [30]. In the present paper, it corresponds to the connectivity between the solid phases (considered to be the anhydrous cement and the hydrates).

Furthermore, in order to obtain a truly predictive concrete behavior model, the formulation and, more particularly, the water to cement ratio w/c must be taken into consideration. Bernard et al.

[5] proposed a threshold α_0 that varied with the w/c ratio, observing that the grains of cement suspended in water percolated for a given value of degree of hydration. In qualitative terms, this is in good agreement with Taplin's experimental results (reported by Byfors [1]) obtained on cement pastes with various w/c ratios, provided that the w/c ratio is relatively high (Fig. 6).

For high w/c ratio values in a cement paste, an important quantity of hydration products is required in order to reach the percolation threshold (see Fig. 7A). For low w/c ratio values, anhydrous grains are closer one to another, and then only a small quantity of hydration products needs to be formed in order to achieve percolation (see Fig. 7B). As anhydrous cement grains have higher mechanical properties than the hydration products, the theory is in good correlation with Taplin's experimental results. It should be pointed out that percolation (in the *mechanical* sense) is not reached if there is a solid percolation which involves only anhydrous cement grains. Indeed, in this case, there is no cohesion in the material which behaves like sand.

A "burning" algorithm can be used in order to detect and monitor percolation. Using the same model for generating the microstructure, the "fire" is started on the left side of the REV. The anhydrous cement and the hydration products located on the border are considered to be part of the percolating path. Then, the "fire" spreads under certain conditions: from a hydration product to an anhydrous cement grain (and vice versa) and from one hydration product to another. At the end, one obtains the percolated cluster that participates to the cohesion and stiffness of the cement paste for a given degree of hydration. An example of the microstructure and its associated percolated cluster is given in Fig. 8.

Several simulations on 2D and 3D microstructures (Fig. 9) of different sizes were initially carried out, in order to evaluate the influence of the REV size on the obtained results. In the 2D case, microstructure ranging between 25×25 and 300×300 pixels were generated; it was observed that the percolation threshold is lower for the smaller microstructures, but beyond a REV of 90×90 elements, the value of the percolation threshold remains almost unchanged (see Fig. 10). Computations were thus performed considering a 90×90 microstructure, and 20 simulations for each selected w/c ratio and degree of hydration combination were performed.

In the 3D case, microstructures with 5000, 40,000 and 125,000 voxels, having different slenderness ratios (0.16, 1, 5, and 40) were compared. The 125,000-element microstructures exhibit almost the same percolation threshold, irrespective of the slenderness ratio (SL). The 5000- and 40,000-element microstructures are more prone to variations of the percolation threshold function of the SL value. In Fig. 11, the variation of the percolation probability (PP) with the degree of hydration for different SL values is illustrated. For the two extreme slenderness ratios (0.16 and 40), the percolation threshold is sensitive to the number of the elements in the microstructure. In the case of a SL value equal to 1, all microstructures show the same percolation threshold. Still, a significant

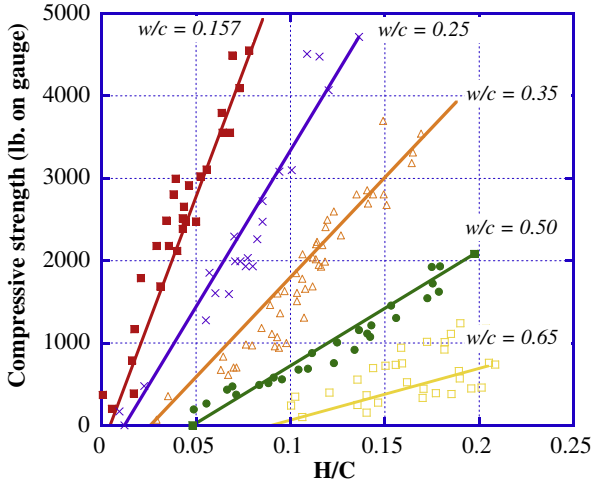

Fig. 6. Changes in compressive strength of cement pastes of various w/c ratios – Taplin's experiments (quoted by Byfors [1]). The ratio H/C represents the amount of hydration products per gram of cement. The compressive strength is reported as lb. on gauge, since the effective area of the specimen under test was not known.

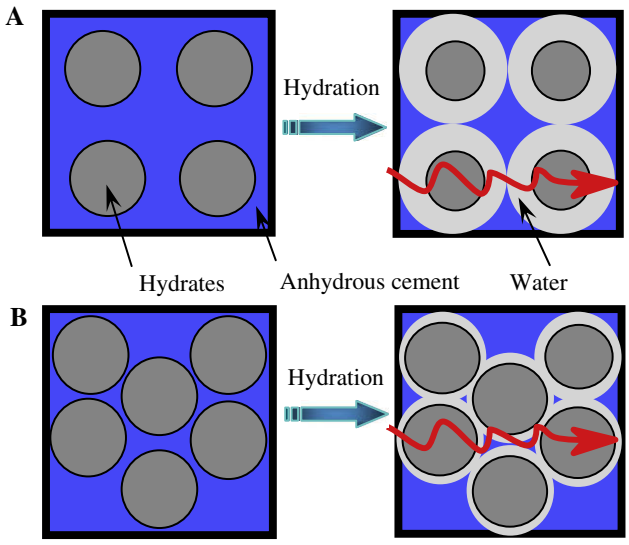

Fig. 7. Schematic representations of hydration and mechanical percolation.

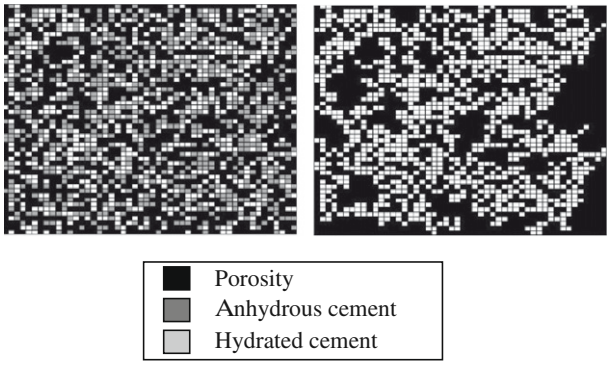

Fig. 8. Generated microstructure and percolated cluster for a $w/c = 0.5$ and $\alpha = 0.28$.

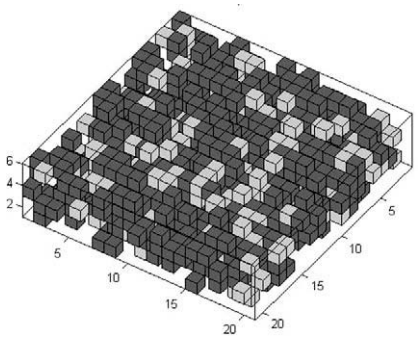

Fig. 9. 3D generated microstructure for a $w/c = 0.6$ and $\alpha = 0.15$ (section through a $20 \times 20 \times 100$ microstructure).

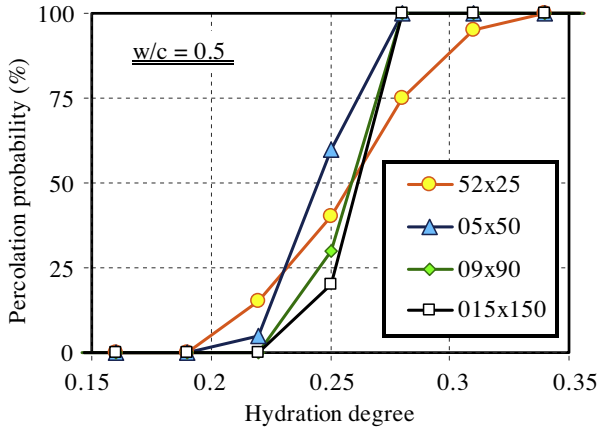

Fig. 10. Percolation probability for two dimensional microstructures.

degree of hydration must be reached in order to attain the percolation threshold for all simulated microstructures that are tested (100% percolation probability for a 40,000-element microstructure reached for $\alpha_{100\%} = 0.22$ versus $\alpha_{100\%} = 0.08$ for a SL = 5). In the case of a SL value equal to 5, all investigated microstructures percolate at the same moment. Moreover, the 100% percolation probability does not differ much either. At the moment when all microstructures have percolated (100% PP), the Young's modulus value is very low, as it can be seen in Table 2. Therefore, the number of elements of the microstructure does not influence much the calculated values.

Taking into account the latter observations, and considering the fact that the time required for calculation in the case of microstructures having 125,000-elements can be very important, especially for low *w*/*c* ratios, the computations of the elastic properties were performed on 40,000-element microstructures, with a SL value equal to 5.

Table 2
Young's modulus at 100% PP.

Number of elements in the microstructure	$\alpha_{100\%}$	*E* (GPa)
5000	0.12	0.38
40,000	0.08	0.22
125,000	0.1	0.15

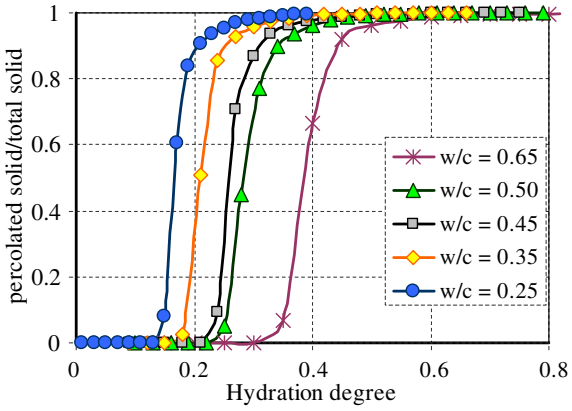

Fig. 12. Percolated solid/total solid grains in the microstructure with respect to the degree of hydration for different *w*/*c* ratios (2D microstructures).

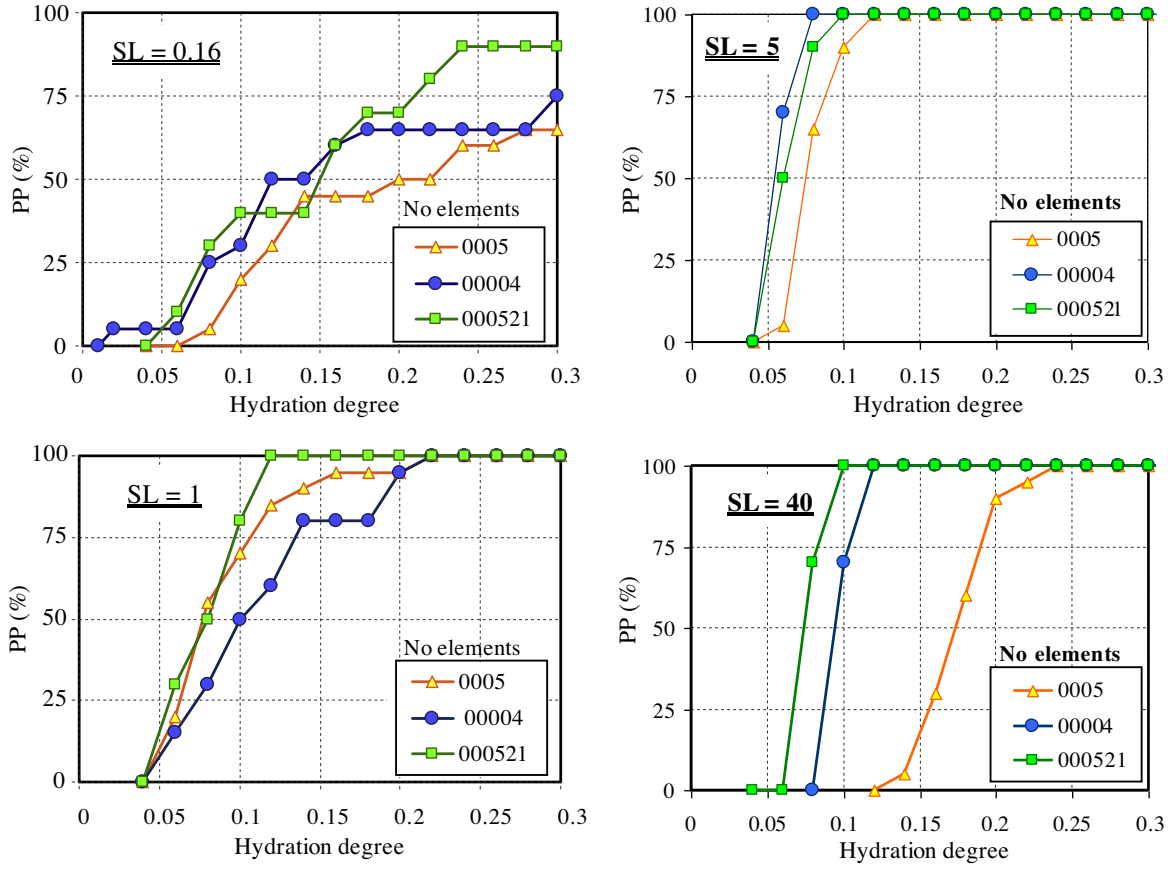

Fig. 11. Percolation probability (PP) for three dimensional microstructures, function of the slenderness ratio (SL).

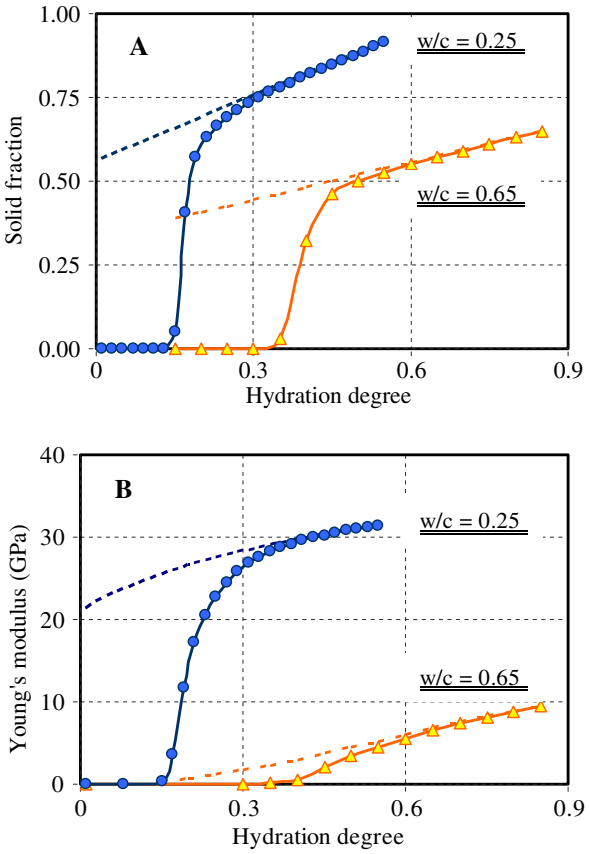

Fig. 13. 2D calculation (SCS): (A) Evolution of the solid fraction; and (B) Evolution of Young's modulus with the degree of the hydration. Entire non-percolated microstructure (dotted line) and percolated cluster (continuous line).

The influence of the water to cement ratio on the percolation threshold is clearly illustrated in Fig. 12. The threshold value increases with the w/c ratio, which is in accordance with the experimental observations.

In Fig. 13A, it can be seen that the evolution of the solid fraction (anhydrous cement and hydrates) with respect to the advancement of hydration in the entire (non-percolated) microstructure (dotted line) and in the percolated cluster (continuous line). It can be seen that in the case of the percolated cluster, the solid fraction is being taken into account only after the percolation threshold appears. This translates on Fig. 13B the fact that the calculation performed on the non-percolated microstructure yields non-zero values of Young's modulus for a zero degree of hydration, as shown in Section 4. Ultimately, for high degrees of hydration, the curves converge, and for $\alpha = \alpha_{max}$ the Young's modulus values are identical.

The difference between 3D and 2D calculations lies in the fact that the percolation threshold is significantly higher in the case of 2D microstructures (Fig. 14A and B). This influences the results obtained for Young's modulus, as for low degrees of hydration smaller values in the case of 2D computations are obtained (Fig. 14C). Indeed, percolation occurs later in 2D calculations, as expected. For higher degrees of hydration the difference becomes negligible.

6. Results

The computation methods described in Section 3 (finite element method and homogenization) are applied, but this time only on the percolated cluster. The solid particles that are not found on the percolation path are not taken into consideration in the computation of mechanical properties, as they are considered to be part of the porosity (solids in suspension).

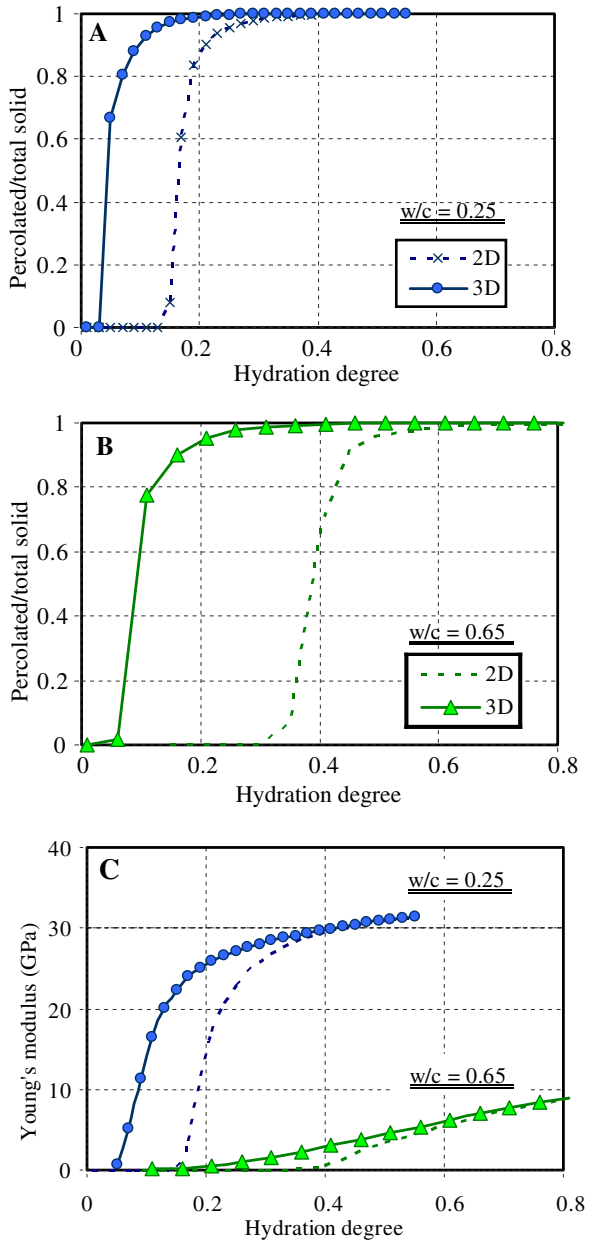

Fig. 14. (A and B) Percolated solid/total solid grains as a function of the degree of hydration for $w/c = 0.25$ and $w/c = 0.65$; (C) Evolution of Young's modulus with the degree of the hydration (SCS). 2D microstructure (dotted) and 3D microstructure (continuous).

In Fig. 15 it can be seen that with the burning algorithm, the finite element calculations give realistic results, since until the percolation threshold is reached, no microstructure shall be generated and imported in the FEM code. Once the first path of connected particles is detected, the FEM calculations can be undertaken.

Still, the finite element calculations are influenced by several factors. First, the base element used for the initial mesh was an 8-nodes quadrangular element. By replacing it with other types of finite elements (4-nodes quadrangular element, 3-nodes triangular element or 6-nodes triangular element), different Young's modulus values are obtained. The obtained results are plotted along with the results obtained by applying the analytical method on the same microstructure (self-consistent scheme – SCS, Fig. 16).

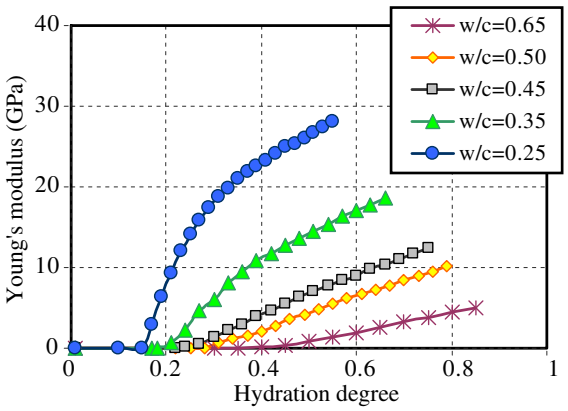

Fig. 15. FEM calculation performed on the percolated cluster: evolution of Young's modulus with the degree of hydration (2D calculation).

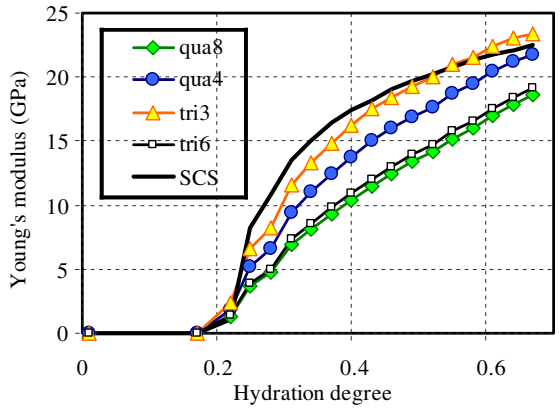

Fig. 16. FEM calculus performed on the percolated cluster: influence of the type of element used on the evolution of Young's modulus ($w/c = 0.35$).

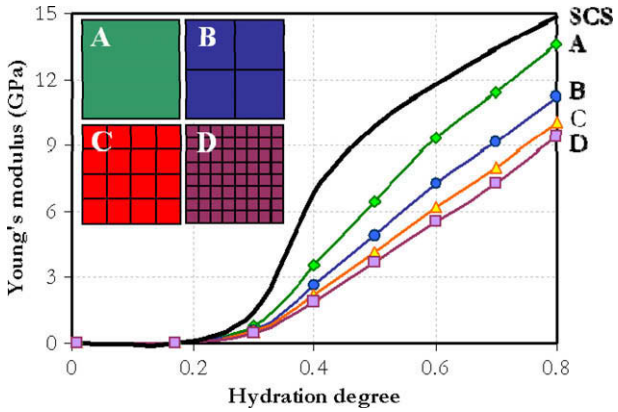

Fig. 17. FEM calculation performed on the percolated cluster: influence of the refinement of the mesh on the evolution of Young's modulus (4-nodes quadrangular elements, $w/c = 0.50$).

Moreover, the results are also influenced by the refinement of the mesh, as shown in Fig. 17. Each pixel of the same microstructure is refined into 4, 16 or 64 elements. The approach is time-consuming, and demands important memory resources. For comparison, results obtained with analytical methods are also plotted on the same graph.

The self-consistent scheme was applied on the same percolated cluster that was used in the case of the finite element calculations. The results are presented in Fig. 18. The values for the final Young's

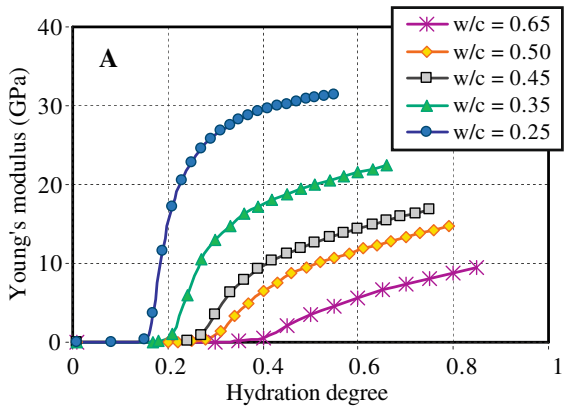

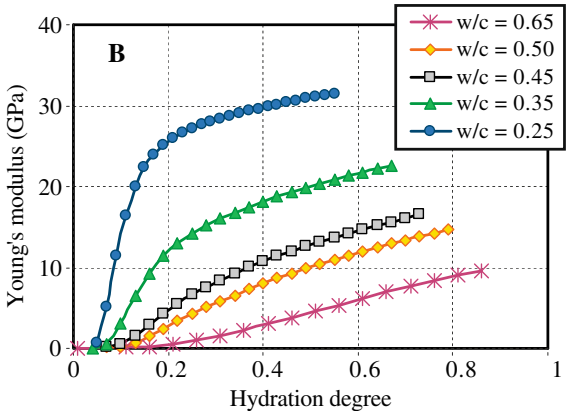

Fig. 18. SCS applied on the percolated cluster: evolution of Young's modulus with respect to the degree of hydration: (A) 2D calculus; (B) 3D calculation.

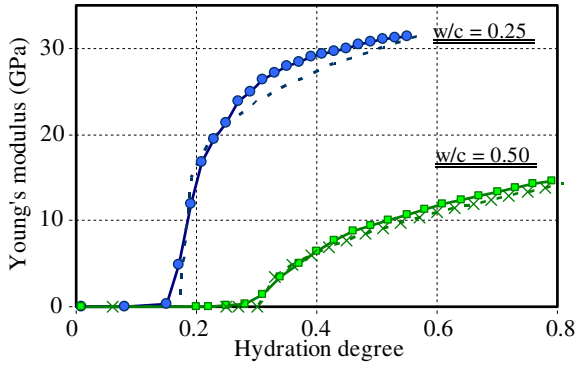

Fig. 19. Evolution of Young's modulus: comparison between Eq. (10) (dotted) and the SCS results (continuous) with $\beta = w/c$.

modulus are higher in the case of the SCS. This does not come as a surprise, as it was already shown that a 2D finite element computation is prone to errors and underestimates the Young's modulus [31].

A comparison can be made between the results obtained using Eq. (10), which describes the phenomenological evolution of Young's modulus, and the SCS computations (Fig. 19). It can be observed that, provided the input values for α_0, E_c (α_{max}) and β are accurate, the predicted evolution is very similar to that obtained with the SCS approach. This supports the use of Eq. (10) as a simplified approach in modeling the evolution of the mechanical behavior of concrete for high degrees of hydration, as it provides a quick and simple prediction of Young's modulus. Still, when it

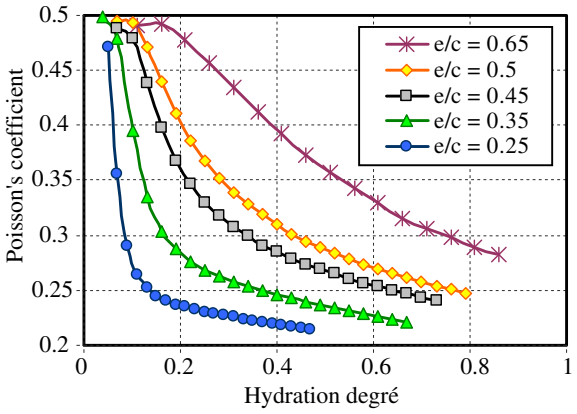

Fig. 20. SCS applied on the percolated cluster: evolution of Poisson's ratio with respect to the degree of hydration (3D calculus).

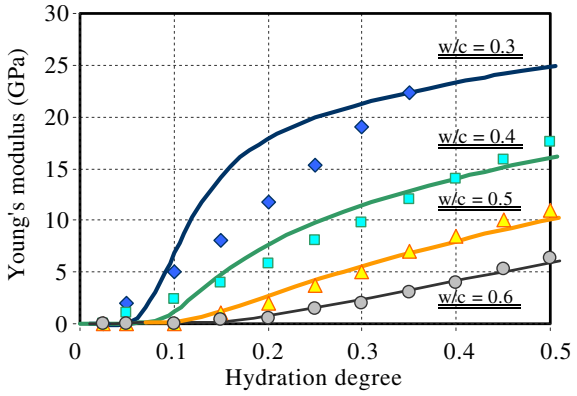

Fig. 21. Early age experimental results [33] (points) versus 3D calculus results (continuous lines).

comes to early age evaluation of mechanical properties, Eq. (10) cannot reproduce the inflection point found in the vicinity of the percolation threshold.

The use of the homogenization method yields a large quantity of information concerning the mechanical properties of the evolving microstructure. In Fig. 20, the evolution of the Poisson's coefficient as a function of the degree of hydration, is presented for several water to cement ratios. At the beginning, the cement particles are in suspension in the water solution and the Poisson's ratio values are close to 0.5. As the hydration process goes on, water is consumed and replaced progressively by solid compounds. The Poisson's ratio decreases with hydration, down to values ranging between 0.25 and 0.15, which are typically reported for hardened cement-based materials.

The results yielded by the homogenization method combined with the percolation algorithm on 3D microstructures are compared to experimental data found in literature. At early age, measures of static Young's modulus, plotted function of the degree of hydration, are scarce. In Fig. 21, dynamic values of Young's modulus, obtained by Boumiz [33] for cement pastes of different water to cement ratios using ultrasonic measurements, versus the values obtained with the model presented, are illustrated. There are several points that need to be emphasized. Firstly, the percolation threshold seems to be consistent with the results obtained experimentally for the higher water to cement ratios. Still for lower water to cement ratios, the experimental percolation threshold is lower. The reason for this is that measure will acquire data as soon as solid parts come in contact one with another, no matter if the solid concerned is formed by anhydrous grains or hydrates. For

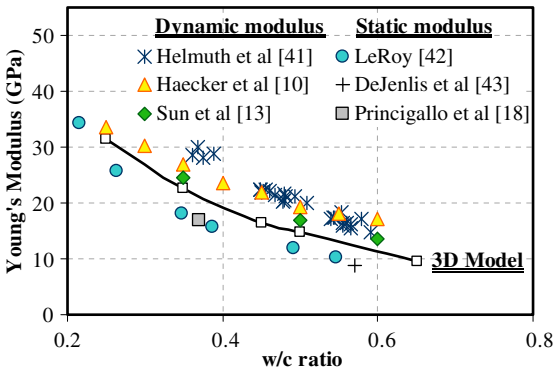

Fig. 22. Experimental results (points) versus 3D calculus results (continuous lines) at complete hydration. (See above mentioned references for further information.)

low water cement ratio, the grains are closely stacked together, so the chances that anhydrous grains are in contact are higher. The model considers a percolation threshold only in the case of a path of solids bonded together by the hydrates, so a higher degree of hydration needs to be reached. In the case of higher water to cement ratios, the solid particles are loosely distributed, so direct contacts between anhydrous cement grains are seldom. The need of forming a sufficient hydrated layer in order to reach the percolation threshold is thus perceived by the ultrasonic measure. At later ages, a linear relation between the evolution of Young's modulus and the degree of hydration can be observed in the case of experimental results. For low water to cement ratios, the model is no longer consistent with the experimental evolution. Several experimental observations show that the evolution of Young's modulus is more likely to have an exponential form, rather than a linear one [6,32] with a rapid increase in the first 24 h [34,35], and a deceleration in the following days. For the 0.3 water to cement ratio it is easily observed that the linear relation obtained experimentally implies a steady evolution of the Young's modulus even after the first day. This translates in systematically higher results obtained for the dynamic modulus versus the classical static measure, in the case of hardened materials [36,1,6]. The results yielded by the model, for a maximal degree of hydration (α_{max} computed accordingly to Eq. (4)) are plotted against experimental data for hardened cement pastes. It can be observed that the dynamic modulus displays higher values than static measures (Fig. 22). The values obtained by the homogenization method are found in the interval between the static and dynamic measures. This comes as a consequence of the limitations of Power's model. Firstly, as the hydrates are seen as a global entity, and the proportions of mineralogical components of anhydrous cement grains are not an input in the calculation, it is difficult to have a precise evolution of each phase. This brings a certain lack of precision, as the

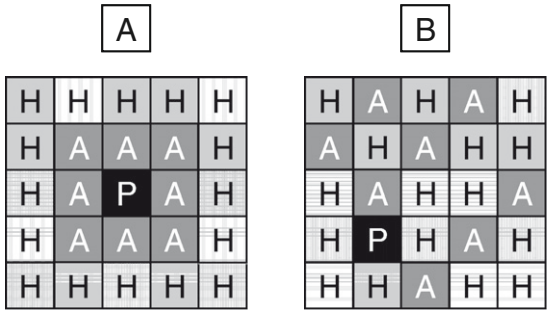

Fig. 23. (A) theoretical disposition of different phases in the microstructure (SCS). (B) Actual phase distribution in the generated microstructure. (P = porosity, A = anhydrous grains, H = cement paste).

model cannot take into account the type of cement used, so comparison with experimental data can be affected. Although the use of Power's model [17] presents several downsides, it also grants the advantage that it allows a rapid estimation of the evolution of the volumetric fractions in the microstructure, yielding results reasonably close to more complex models.

7. Discussions and conclusions

It has been shown that neither the self-consistent scheme homogenization nor finite element computations enable an accurate prediction of Young's modulus evolution in low w/c ratio cement-based materials as a function of the degree of hydration. In the case of w/c values lower than 0.32, non-zero Young's modulus values are yielded right from the initial water-to-cement contact (degree of hydration equal to zero), as both methods fail to account for the moment of transition between the fluid and solid states. Even if the SCS provides a percolation threshold for a solid fraction of 50%, this is not sufficient. For a perfect cluster of spheres, theoretical percolation threshold in 2D is reached for a solid fraction of 59.3%, whereas in 3D, the corresponding value is 30.7%. Still, the percolation threshold of cementitious materials depends on the w/c ratio. Last, but not least, the computations on the entire (non-percolated) microstructure are highly time-consuming.

The setting phenomenon which arises in cementitious materials and the subsequent binding role of the hydrates can be modeled by using a burning algorithm. A percolated cluster is thus obtained and the computation methods can then be applied by considering only to the solid fraction of this cluster.

The SCS approach applied to the percolation cluster appears to yield consistent results. Yet, since the method is based on the assumption that the different phases evolve concentrically, the simulated microstructure should exhibit a phase distribution somewhat similar to that shown in Fig. 23A. On the contrary, in this study, the microstructure is generated randomly and the various phases are distributed accordingly (Fig. 23B). Further investigations, using refined microstructural models, are expected to provide valuable information concerning the extent of applicability of the SCS.

Besides, applying the FEM calculation approach to the percolated cluster results in a realistic prediction of the material mechanical properties with time. The results, however, depend to a great extent on the type of elements used and on the REV mesh refinement. Moreover, by using a simple phenomenological approach, a rather close evolution is predicted.

The proposed approach could be applied on more refined microstructures, using advanced hydration models (as Cemhyd3D or Hymostruc), in order to have an accurate representation of the cement paste.

References

[1] J. Byfors, Plain concrete at early ages, PhD Thesis, Swedish cement and concrete institute, Sweden 1980.
[2] J.-M. Torrenti, Bulletin de Liaison des LPC 179 (1992) 31–41.
[3] G. de Schutter, L. Taerwe, Materials and Structures 29 (1996) 335–344.
[4] E.J. Garboczi, D.P. Bentz, K.A. Snyder, N.S. Martys, P.E. Stutzman, C.F. Ferraris, J.W. Bullard, An Electronic Monograph: Modelling and Measuring the Structure and Properties of Cement-Based Materials, 2003 <http://ciks.cbt.nist.gov/garbocz/>.
[5] O. Bernard, F.J. Ulm, E. Lemarchand, Cement and Concrete Research 33 (9) (2003) 1293–1309.
[6] M. Krauβ, K. Hariri, Cement and Concrete Composites 28 (2006) 299–396.
[7] J.H. Hattel, J. Thorborg, Applied Mathematical Modelling 27 (2003) 1–26.
[8] D.P. Bentz, 'CEMHYD3D: a three-dimensional cement hydration and microstructure development modelling package, version 2.0.', NISTIR 6485, US Department of Commerce, 2000, <http://ciks.cbt.nist.gov/monograph>.
[9] K. van Breugel, Simulation of hydration and formation of structure in hardening cement-based materials, PhD Thesis, Technical University Delft, Netherlands, 1997.
[10] C.-J. Haecker, E.J. Garboczi, J.W. Bullard, R.B. Bohn, Z. Sun, S.P. Shah, T. Voigt, Cement and Concrete Research 35 (2005) 1948–1960.
[11] F. Bernard, S. Kamali-Bernard, W. Prince, Cement and Concrete Research 38 (2008) 449–458.
[12] S.J. Lokhorst, K. van Breugel, Cement and Concrete Research 27 (10) (1997) 1465–1479.
[13] Z. Sun, G. Ye, S.P. Shah, ACI Materials Journal 102 (2) (2005) 122–129.
[14] J. Sanahuja, L. Dormieux, G. Chanvillard, Cement and Concrete Research 37 (2007) 1427–1439.
[15] V. Šmilauer, Z. Bittnar, Cement and Concrete Research 36 (2006) 1708–1718.
[16] J.M. Torrenti, F. Benboudjema, Materials and Structures 38 (277) (2005) 299–304.
[17] T.C. Powers, T.L. Brownyard, Journal of the American Concrete Institution 43 (Oct. 1946 to April 1947).
[18] A. Princigallo, P. Lura, K. van Breugel, G. Levita, Cement and Concrete Research 33 (2003) 1013–1020.
[19] E.J. Garboczi, D.P. Bentz, in: Materials Research Society Symposium Proceedings, San Francisco, Materials Research Society, Pittsburgh, 1998, pp. 89–100.
[20] V. Waller, Relations entre composition des bétons, exothermie en cours de prise et résistance en compression. Thèse de doctorat, Ecole Nationale des Ponts et Chaussées, Paris, France, 1999.
[21] Cast3M, CEA <http://www-cast3m.cea.fr/cast3m/index.js>.
[22] K. Velez, S. Maximilien, D. Damidot, G. Fantozzi, F. Sorrentino, Cement and Concrete Research 31 (4) (2001) 555–561.
[23] G. Constantinides, F.-J. Ulm, Cement and Concrete Research 34 (2004) 67–80.
[24] J.D. Eshelby, Proceedings of the Royal Society of London, Series A 241 (1957) 376–396.
[25] I.O. Yaman, H.M. Aktan, N. Hearn, Materials and Structures 35 (2002) 110–116.
[26] Y. Benveniste, Mechanics of Materials 6 (1987) 147–157.
[27] L. Stefan, F. Benboudjema, J.-M. Torrenti, 2D mechanical percolation in cement pastes at early age, in: 2nd International RILEM Symposium September 11–13 2006, Quebec, Canada, CD-ROM.
[28] L. Stefan, J.M. Torrenti, F. Benboudjema, Mechanical threshold of cementitious materials at early age, in: Euro-C Conference on Computational Modelling of Concrete Structures, 2006.
[29] P. Acker, Comportement mécanique du béton: apports de l'approche physico-chimique, Thèse de doctorat, Ecole Nationale des Ponts et Chaussées, France, 1988.
[30] J.W. Bullard, M. D'Ambrosia, Z. Grasley, W. Hansen, N. Kidner, D. Lange, P. Lura, T.O. Mason, J. Moon, F. Rajabipour, G.S. Sant, S. Shah, T. Voigt, N. Wansom, W.J. Weiss, L. Woo, A Comparison Of Test Methods For Early-Age Behavior Of Cementitious Materials, Advances in Concrete through Science and Engineering, RILEM Quebec abstract, p. 307 (electronic proceedings p. 20), 2006.
[31] E. Guillon, Durabilité des matériaux cimentaires – modélisation de l'influence des équilibres physico-chimiques sur la microstructure et les propriétés mécaniques résiduelles, PhD Thesis, Ecole Normale Supérieure de Cachan, 2004.
[32] S. Staquet, C. Boulay, N. Robeyst, N. De Belie, Ultrasonic monitoring of setting and autogenous shrinkage developement of high performance concrete, in: Proceedings of the 8th International Conference on Creep, Shrinkage and Durability of Concrete and Concrete Structures Concreep 8, Ise-Shima, Japan, 2008.
[33] A. Boumiz, Étude comparée des évolutions mécaniques et chimiques des pâtes de ciment et mortiers à très jeune âge, PhD Thesis, Université Paris 7, 1995.
[34] J. Bisschop, Evolution of solid behavior, Report of Rilem Technical Committee TC 181 – EAS early age shrinkage induced stresses and cracking in cementitious systems, vol. 25, 2003.
[35] Y. Kasai, K. Yokoyama, I. Matsui, Tensile properties of early age concrete, in: Proceedings of the 1971 International Conference on Mechanical Behaviour of Materials, vol. IV, 1971.
[36] F. Martinez, Y. Cabrera, Materials and Structures 25 (1992).
[37] H.M. Jennings, P.D. Tennis, Journal of the American Ceramic Society 77 (1994).
[38] O. Laurence, La fissuration due au retrait restreint dans les réparations minces en béton: apports combines de l'expérimentation et de la modélisation, PhD Thesis, École Nationale des Ponts et Chaussées, Université Laval, 2001.
[39] H. Le Chatelier, Sur les changements de volume qui accompagnent le durcissement des ciments, Bulletin de la Société pour l'Encouragement Industriel National V (5ème série), 1900.
[40] G. Ye, K. van Breugel, A.L.A. Fraaij, Cement and Concrete Research 33 (2003).
[41] R. Helmuth, D. Turk, Symposium on Structure of Portland Cement and Concrete (1966) 135–144.
[42] R. Le Roy, Déformations instantanées et différées des bétons à hautes performances, PhD Thesis, Laboratoire Central des Ponts et Chaussées, 1996.
[43] N. deJenlis, Etude des caractéristiques hydriques et mécaniques duciment du bâtiment réacteur de la centrale nucléaire de Civaux, Mémoire deMaster 2, 2008.